Electronic Structure and Hybridization Effects of Zirconium Alloy in High Temperature Water

Taeho Kim[a], Seunghyun Kim[a], Yunju Lee[a], and Ji Hyun Kim[a,*]

[a] School of Mechanical, Aerospace and Nuclear Engineering Ulsan National Institute of Science and Technology (UNIST), Ulju-gun, Ulsan 44919, Republic of Korea
[*]Corresponding author: kimjh@unist.ac.kr

1. Introduction

Zirconium and its alloy have low thermal neutron capture cross section and excellent mechanical properties; therefore, they are used as nuclear fuel cladding materials in nuclear power plants. The phase of zirconium oxide contributes to mechanical properties and corrosion behaviors of zirconium oxide. To assure the safety of nuclear power plants, therefore, the oxidation characteristic and phase of zirconium oxide should be comprehensively understood.

Investigation based diffraction studies has shown that due to the compressive stresses, tetragonal phase fraction is the highest near the oxide/metal interface, where the compressive stress is relatively higher than the middle of the zirconium oxide. As oxidation time increases, the proportion of monoclinic zirconium oxide increases while that of tetragonal zirconium oxide decreases [1–3].

Detailed characterization of the oxide structure and the tetragonal phase fraction using high-energy synchrotron X-ray diffraction on zirconium alloys and metastable tetragonal phase fraction is previously reviewed: The previous study has shown that X-ray absorption spectra are sensitive to the thin film structure [4].

However, the oxidation of zirconium alloys is a complex process, which starts by the alloy developing a black protective oxide resulting in a parabolically decreasing oxidation rate [5]. To identify structure of the zirconium oxide, and the oxide/metal interface, electron energy loss spectroscopy, and atom probe tomography have identified a layer zirconium oxide before the first abrupt transition [6,7].

In this study, a specific zirconium alloy was oxidized and investigated with scanning transmission X-ray microscopy (STXM) for 100 d oxidation, which is close to the first transition time of the zirconium alloy oxidation. The ex situ investigation methods such as transmission electron microscopy (TEM) was used to further characterize the zirconium oxide structure.

2. Experimental

2.1 Materials and specimen preparation

A plate of the zirconium alloy, provided by KEPCO Nuclear Fuel Co., Ltd., was used for the oxidation experiment in the primary water chemistry of pressurized water reactor. The chemical composition of the zirconium alloy is presented in Table. I.

Table. I Chemical composition of zirconium alloy

Element	Nb	Sn	Fe	O	N	C	Zr
Composition (wt. %)	0.96	0.76	0.18	0.62	0.03	0.1	Bal.

The specimens were polished before oxidation. Grits 400 to 800 SiC papers were used to polish the specimen. Next, diamond pastes of up to 1 μm and colloidal SiO_2 were used for minimizing the mechanical transformation of specimens.

2.2 Experimental system

For simulating the primary water chemistry of a pressurized water reactor, a loop and an autoclave for high temperature and pressure conditions were used. The detailed explanation about the system is illustrated in the authors' previous study [8].

Using this system, the conditions of the simulated primary water environment were set as follows: temperature of 360 °C, pressure of 19 MPa, dissolved oxygen concentration of below 5 ppb, and boric acid and lithium hydroxide concentrations of 1200 ppm and 2 ppm, respectively. Also, the dissolved hydrogen concentration is controlled as 30 cm^3/kg. These water chemistry conditions were maintained during the oxidation process, for a total of 100 d.

For STXM experiment, the focused ion beam method is used to make analysis sample. To prevent the surface contamination from impurities and ion beam damage during the FIB process, the specimen surface was coated with sputtered carbon before gallium ion milling.

The structural properties were examined by using the synchrotron X-ray at soft X-ray Nanoscopy beamline (10 A beamline of Pohang Light Source, South Korea). Local electronic structure of the oxidized zirconium samples was investigated by using X-ray absorption fine structure spectroscopy at the O K-edge, and the energy range of O K-edge is set as 520 to 560 eV.

Then, for further investigation of microstructure of zirconium oxide, TEM analysis was conducted for oxidized zirconium alloy for 30, 50, 80 and 100 d.

3. Results and Discussion

3.1. STXM analysis of oxidized zirconium alloy.

The STXM results of oxidized zirconium alloy with different oxidation time are illustrated in Fig. 1. Fig. 1 shows the STXM images of oxidized zirconium alloy cross-section from FIB sampling.

(a) (b)

(c) (d)
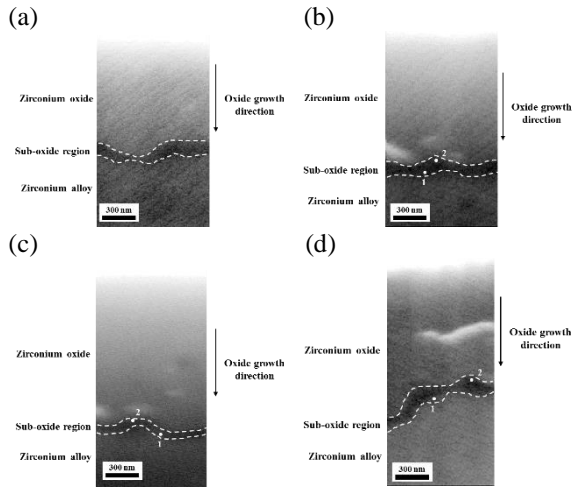
Fig. 1 STXM images of oxidized zirconium alloy (a) 30 d, (b) 50 d, (c) 80 d, and (d) 100 d.

Fig. 1 shows the STXM images of oxidized zirconium alloy with different oxidation time. All STXM image shows the dark-contrast region which existed just above the oxide/metal (O/M) interface. For investigating the characteristic of dark-contrast region, the X-ray absorption spectroscopy of O K-edge energy region was conducted.

X-ray absorption spectroscopy of O K-edge energy region.

(a) 30 d

(b) 50 d

(c) 80 d

(d) 100 d
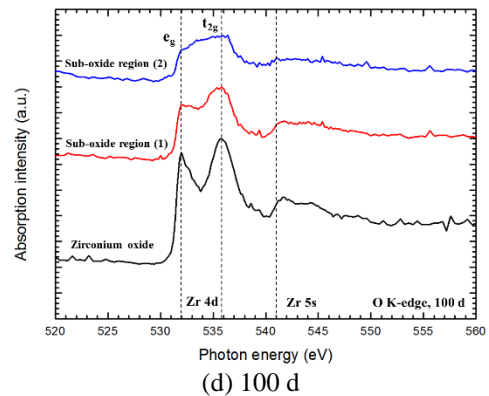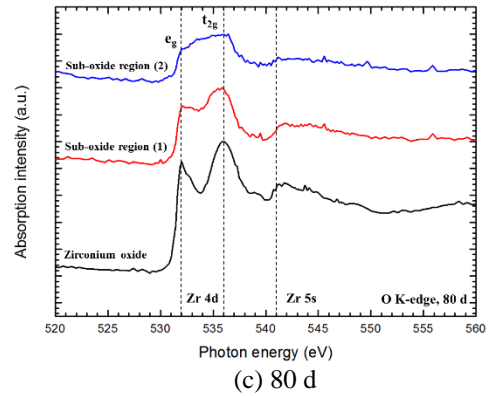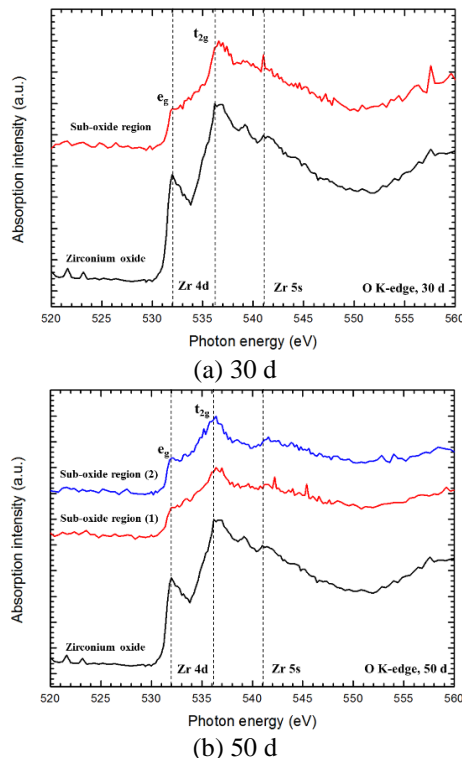
Fig. 2 O K-edge XAS images of oxidized zirconium alloy with different oxidation time

When obtaining the O K-edge XAS spectra in Fig. 2, the oxide/metal interface is assumed just above the metal layer, and the interface is dark area in the 534 eV image, Fig. 1. From the all STXM image, the O/M interface layer thickness is below 100 nm.

The obvious twin peaks are observed in the XAS spectrum of zirconium oxide. The twin-peak structure of the O K-edge means the t_{2g} and e_g orbital of the oxygen are shown in the XAS image. In the electronic structure of ZrO_2 the lowest unoccupied molecular orbitals will be associated with the empty 4d orbitals of the Zr atoms. As a consequence of electron-electron interactions, the latter pair, labeled e_g, are lowered in energy while the former group, labeled t_{2g}, are raised in energy.

The e_g orbital points toward the interstitial sites of zirconium oxide between the two oxygen atoms, hence is "nonbonding," while t_{2g} orbital is "bonding" [9].

The first peak ($\sim$532 eV) corresponds to the excitation from the O 1s state to the hybridized O 2p−Zr 3d state, and the second ($\sim$536V) and third peaks ($\sim$541 eV) have been attributed to the excitations of O 1s to O 2p−Zr 5d, and O 2p−Zr 4sp, respectively.

This results show that the oxygen chemistry is different in sub-oxide region compared to the bulk zirconium oxide layer. Two sharp peaks which can be contributed to the e_g and t_{2g} disappear as far from the bulk oxide. This means the crystal structure of dark-contrast region is different from bulk zirconium oxide. For further investigation of phase of dark-contrast region, the TEM analysis is conducted.

3.2. TEM analysis of oxidized zirconium alloy
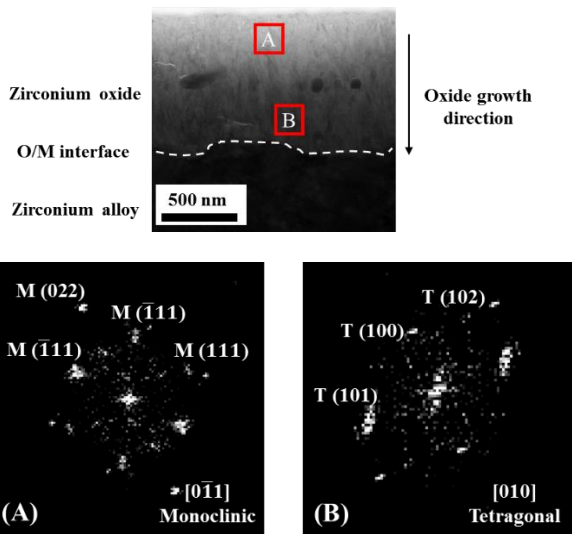
Fig. 3 TEM and FFT analysis results of oxidized zirconium alloy after 30 d oxidation.

(a) 50 d
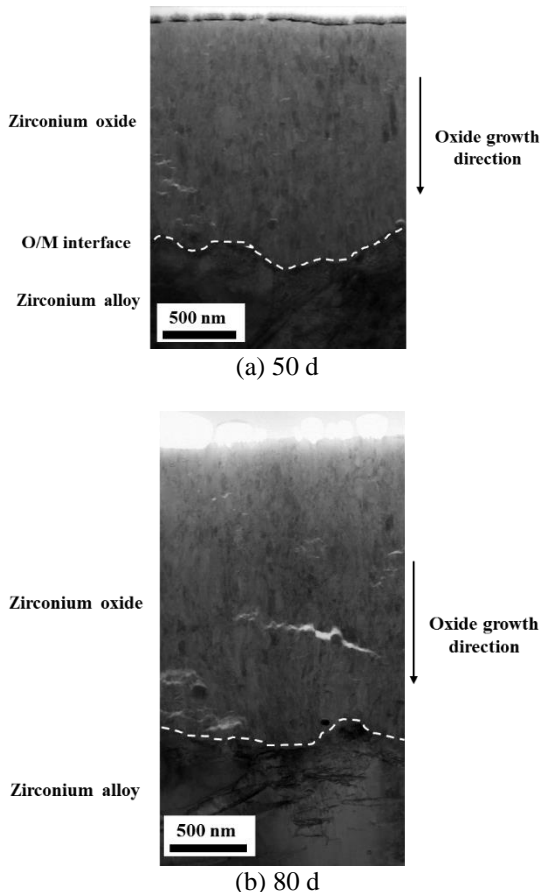
(b) 80 d

Fig. 4 TEM analysis results of oxidized zirconium alloy after (a) 50 and (b) 80 d oxidation.

For investigating the phase of zirconium oxide with different oxidation time, the TEM analysis was conducted. After 30 d oxidation, the oxide thickness increased to 0.88 μm. For investigating the phase of zirconium oxide at specific position, the Fast Fourier transform (FFT) analysis was conducted from positions "A" and "B" which are marked with a red box in Fig. 3. The middle oxide which can be represented as A is analyzed as monoclinic, and the O/M interface, which can be represented as "B" is analyzed as tetragonal zirconium oxide phase. It is well-matched with in situ Raman spectroscopy results. The oxide thickness is below 1 μm; therefore, the tetragonal zirconium oxide peak can be shown in Raman spectrum after 30 d.

Fig. 4 is the TEM image of oxidized zirconium alloy after 50 and 80 d, respectively. The oxide thickness is increased from 1.46 μm to 2.27 μm as oxidation time increases from 50 d to 80 d.

Fig. 5 is the TEM image of oxidized zirconium alloy after 100 d. The oxide thickness is increased to 2.44 μm as oxidation time increases to 100 d. The d-spacing of positions "A", "B", and "C" are explained, and the zirconium oxide phases located at these three sites are determined using JCPDS diffraction reference data (37-1484, 42-114, 50-1087; zirconium oxide). The FFT analysis results show that the oxide phase of positions "A" and "B" are monoclinic zirconium oxide, especially (110) and (120) planes. This means that the top and middle regions of zirconium oxide are monoclinic dominant zirconium oxide. The tetragonal zirconium oxide, which has (102) and (211) planes, is shown in position "C," which represents the O/M interface. It shows that the tetragonal zirconium oxide is always positioned near the O/M interface during the zirconium oxidation process.
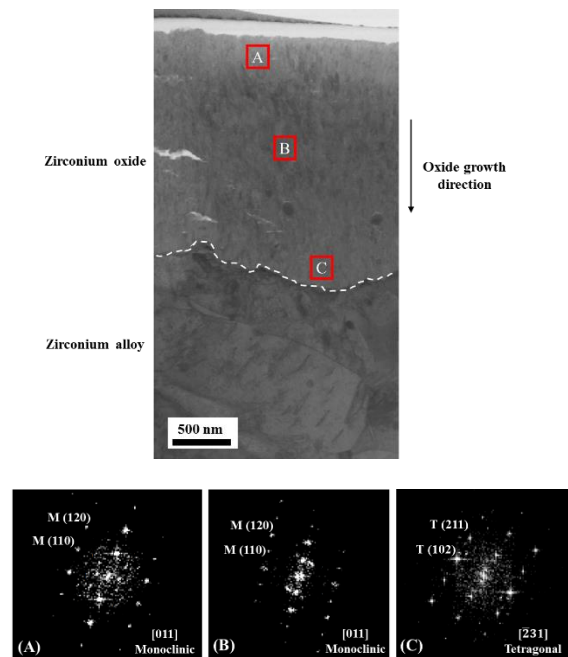
Fig. 5 TEM and FFT analysis results of oxidized zirconium alloy after 100 d oxidation.

3.3 Oxygen chemistry of zirconium oxide

Many previous researches explained that the sub-oxide layer is a metastable ordered solution of O in Zr, although no sub-oxide diffraction peaks could be clearly indexed in TEM [7]. However, small crystallites which can be attributed to the tetragonal zirconium oxide

appear in the rectangular grains in the sub-oxide region. This can explain the tetragonal oxide is found just near the O/M interface, which is included in the sub-oxide region.

From STXM and XAS analysis, the dark-contrast region is existed just above the O/M interface, and thickness of that region is around 50 to 100 nm. This indicates that the oxygen chemistry is different compared to the bulk zirconium oxide. The sharp e_g and t_{2g} orbitals peaks related to the Zr 4d and O 2p hybridization disappear in the sub-oxide region.

TEM analysis results also show that the tetragonal zirconium oxide is positioned just above the O/M interface, and the position of tetragonal zirconium oxide is overlapped with the sub-oxide region. This result is well matched with the previous researches [10,11],

4. Conclusions

In this study, synchrotron STXM and TEM analysis were conducted for investigating the phase transformation of zirconium alloy in primary water. From this study, the following conclusions are drawn:

1. The zirconium alloy was oxidized in primary water chemistry for 100 d, and the STXM and XAS were measured after 30, 50, 80, and 100 d from start-up. The hybridization state of Zr 4d and O 2p orbitals are changed with the position of oxide.

2. As oxidation time increased, the sub-oxide region, which is positioned just above the O/M interface is remained.

3. TEM and FFT analysis showed that the zirconium oxide mostly consisted of the monoclinic phase. The tetragonal zirconium oxide was just found near the O/M interface..

ACKNOWLEDGMENT

REFERENCES

[1] P. Frankel, J. Wei, E. Francis, a. Forsey, N. Ni, S. Lozano-Perez, The effect of Sn on corrosion mechanisms in advanced Zr-cladding for pressurised water reactors, Zircon. Nucl. Ind. 17th. 61 pp. 4200–4214, 2013

[2] A. Garner, A. Gholinia, P. Frankel, M. Gass, I. MacLaren, M. Preuss, The microstructure and microtexture of zirconium oxide films stiudied by transmission electron backscatter diffraction and automated crystal orientation mapping with transmission electron microscopy, Acta Mater. 80 pp. 159–171, 2014

[3] W. Qin, C. Nam, H.L. Li, J. A, Szpunar, Tetragonal phase stability in ZrO2 film formed on zirconium alloys and its effects on corrosion resistance, Acta Mater. 55 pp. 1695–1701, 2007

[4] A. Kikas, J. Aarik, V. Kisand, K. Kooser, T. Käämbre, H. Mändar, Effect of phase composition on X-ray absorption spectra of ZrO2 thin films, J. Electron Spectros. Relat. Phenomena. 156158, pp. 303–306, 2006

[5] R.J. Nicholls, N. Ni, S. Lozano-Perez, A. London, D.W. McComb, P.D. Nellist, Crystal structure of the ZrO phase at zirconium/zirconium oxide interfaces, Adv. Eng. Mater. 17 pp. 211–215, 2015

[6] N. Ni, S. Lozano-Perez, J. Sykes, C. Grovenor, Quantitative EELS analysis of zirconium alloy metal/oxide interfaces, Ultramicroscopy. 111, pp. 123–130, 2010

[7] N. Ni, D. Hudson, J. Wei, P. Wang, S. Lozano-Perez, G.D.W. Smith How the crystallography and nanoscale chemistry of the metal/oxide interface develops during the aqueous oxidation of zirconium cladding alloys, Acta Mater. 60, pp. 7132–7149, 2012

[8] T. Kim, J. Kim, K.J. Choi, S.C. Yoo, S. Kim, J.H. Kim, Phase Transformation of Oxide Film in Zirconium Alloy in High Temperature Hydrogenated Water, Corros. Sci. 99, 134–144, 2015

[9] Y. Lei, Y. Ito, N.D. Browning, T.J. Mazanec, Segregation Effects at Grain Boundaries in Fluorite-Structured Ceramics, J. Am. Ceram. Soc. 85, pp. 2359–2363, 2002

[10] J. Hu, A. Garner, N. Ni, A. Gholinia, R.J. Nicholls, S. Lozano-Perez, et al., Identifying suboxide grains at the metal-oxide interface of a corroded Zr-1.0%Nb alloy using (S)TEM, transmission-EBSD and EELS, Micron. 69, pp. 35–42, 2015

[11] L. Kurpaska, I. Jozwik, J. Jagielski, Study of sub-oxide phases at the metal-oxide interface in oxidized pure zirconium and Zr-1.0% Nb alloy by using SEM/FIB/EBSD and EDS techniques, J. Nucl. Mater. 476, pp. 56-62, 2016